

# Vibrational spectroscopic characterization of lanthanide molybdates

M. DEL C. VIOLA, A. M. SANGRA, J. C. PEDREGOSA

*Departamento de Química Inorgánica "Dr. Gabino F. Puelles", Facultad de Química, Bioquímica y Farmacia, Universidad Nacional de San Luis, 5700-San Luis, Argentina*

The vibrational spectrum of lanthanide molybdates (materials with important optical, electrical and catalytic properties) was assigned by using sites symmetry and factor group analysis. Raman and infrared spectra were registered and the modes corresponding to the  $\text{MoO}_4^{2-}$  and  $\text{LnO}_n$  polyhedra were specified. An interesting behaviour for the symmetric stretching mode of the molybdate ion was found in these condensed lattices. The lanthanide cation does not influence the  $\text{MoO}_4^{2-}$  vibrational behaviour. The use of this spectroscopy to characterize these materials is thus shown.

## 1. Introduction

Lanthanide molybdates present interesting optical, electrical and catalytic properties [1–4]. All these compounds crystallize in two typical structures with different dispositions of the lattice constituent polyhedra.

Recently we have studied the spectroscopic behaviour of condensed phases and observed strong couplings in the vibrational modes of the polyhedra, which makes a complete assignation difficult [5–7]. We have also analysed the changes in vibrational behaviour in substituting diverse cations in compound lattices with similar applications [8].

Because of their applications, lanthanide molybdates have been characterized by vibrational spectroscopy because no complete data on this behaviour can be found in current literature. We also undertook this work with the purpose of giving a complete assignation of the polyhedra modes existing in each structure, of studying the possible couplings between them and of proving the influence of Ln(III) cation on the molybdate ion vibrations. The usefulness of vibrational spectroscopy in the characterization of these materials is also shown.

## 2. Experimental procedure

Microcrystalline samples of  $\text{Ln}_2(\text{MoO}_4)_3$ , with Ln = La to Lu, were obtained by solid-state reaction at 700 °C, from stoichiometric  $\text{MoO}_3$  and  $\text{Ln}_2\text{O}_3$  mixtures. The fine-powdered mixtures were placed in a platinum crucible and fired in a muffle-furnace at 700 °C in several periods totalling 15 h, with intermediate grindings of the reaction mixture. Samples were characterized by chemical analyses and X-ray powder diffractometry.

X-ray powder diagrams (Debye–Scherrer) were obtained with a Rigaku 2002 Miniflex diffractometer, using nickel-filtered  $\text{CuK}_\alpha$  radiation ( $\lambda = 0.15418 \text{ nm}$ )

and NaCl and quartz as external calibration standards.

Infrared spectra were recorded using a Perkin–Elmer 683 spectrometer using the KBr pellet technique.

Raman spectra were obtained with a Spex–Ramalog 1403 spectrometer equipped with a SCAMP control unit and using the 514.5 nm line of an argon-ion laser for excitation.

## 3. Results and discussion

### 3.1. Structural studies

#### 3.1.1. $\text{Sc}_2(\text{WO}_4)_3$ lattices

Terbium to lutetium molybdates crystallize in this type of structure. They belong to the orthorhombic system, space group  $\text{Pbcn}$  ( $D_{2h}^{14}$ , no 60) where the molybdate ion occupies sites of  $C_1$  symmetry containing four molecules in each unit cell. The structure consists of condensed layers in which the  $\text{MoO}_4$  tetrahedra and  $\text{LnO}_6$  octahedra are joined by their corners. Both polyhedra are regular, not much distorted and they do not contact each other by means of the Mo–O–Mo and Ln–O–Ln bridges [1].

#### 3.1.2. $\text{La}_2(\text{MoO}_4)_3$ lattices

Lanthanum to gadolinium molybdates crystallize in this type of structure. They belong to the monoclinic system, space group  $\text{C}_{2/c}$  ( $C_{2h}^6$ , no 15) with 12 molecules in each unit cell. This is scheelite-like structure with cationic vacancies [10]. Hence, it must be formulated as  $\text{La}_{2/3}\square_{1/3}\text{MoO}_4$ . Each molybdenum is in a tetrahedral environment surrounded by two oxygens at a distance of 0.172 and 0.187 nm. In addition, there is a fifth oxygen at a distance of 0.22 nm near to  $\text{MoO}_4$ . If the coordination of the last oxygen is taken into account, it could be considered that the molybdenums surrounding it is similar to an irregular trigonal bipyramid and in the lattice these polyhedra

share a side, forming  $\text{Mo}_2\text{O}_8$  groups. The Ln(III) ions are in the centre of the polyhedra, surrounded by 8 oxygens with Mo–O–Ln bridges.

Therefore, this structure is more condensed than the former and presents vacancies in the lattice. There also exists further contact among similar polyhedra.

### 3.2. Vibrational spectrum

#### 3.2.1. $\text{Sc}_2(\text{MoO}_4)_3$ lattices

On the basis of structural data, site symmetry and factor group analysis could be carried out to vibrational modes of tetrahedra. Table I shows the corresponding correlation. One band for  $\nu_1$ , two for  $\nu_2$  and three bands for  $\nu_3$  and  $\nu_4$  modes, respectively, are expected by site symmetry, both in infrared and Raman spectroscopy. Additional splittings are expected for the factor group.

Our results coincide with the expectations based on site symmetry analysis and only the  $\nu_3$  mode presents additional splittings for the factor group. Furthermore, vibrations corresponding to the  $\text{LnO}_6$  octahedra are clearly observed. Fig. 1 shows the infrared and Raman spectra of  $\text{Lu}_2(\text{MoO}_4)_3$ , which is characteristic of this series, whereas Table II shows the assignation performed.

The  $\nu_1$  mode corresponding to the  $\text{MoO}_4$  symmetric stretching appears among the components of the  $\nu_3$  antisymmetric mode as a unique, perfectly differentiable band, basically in the Raman spectrum. This becomes a novelty, because earlier studies showed that in some cases  $\nu_1$  appears as in aqueous solutions at higher frequencies than  $\nu_3$  [11] while in others the situation is reversed. Our spectra are conclusive as to the relative position of  $\nu_1$  in this type of structure.

The values of this mode, as in most of the molybdates of trivalent cations [12], vary linearly with the effective nuclear charge of the cation. However, this behaviour is not observed in these molybdates. Table III shows the  $\nu_1$  variation for lanthanides of this series where this anomalous behaviour is seen.

The antisymmetric  $\nu_3$  mode is present in the three components, where site symmetry is expected, presenting additional splittings by the factor group in the infrared and Raman spectra. Couplings between the different polyhedra found in other condensed molyb-

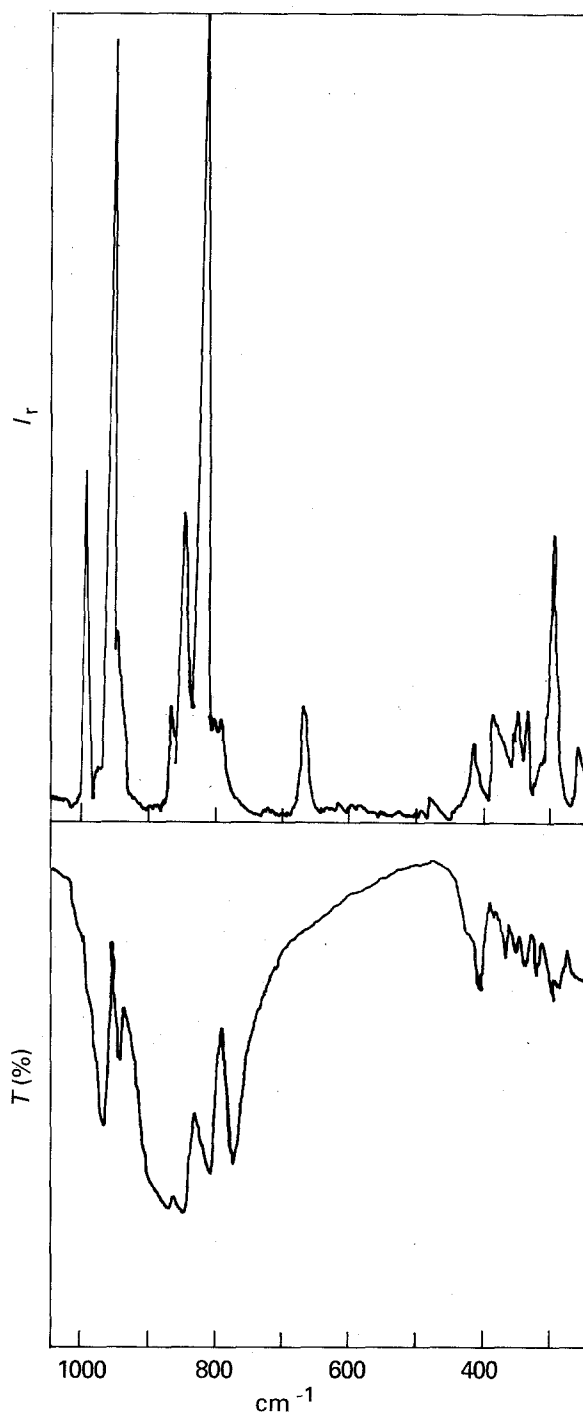


Figure 1 Vibrational spectrum of  $\text{Lu}_2(\text{MoO}_4)_3$ .

TABLE I Correlation between the point group Td, the site group C1 and the factor group D2h

Td	C1	D2h
$\nu_1$ ( $A_1$ ) (R)	A (IR, R)	$\begin{cases} 3(\text{Ag} + \text{B1g}) \text{ (R)} \\ 3(\text{B2u} + \text{B3u}) \text{ (IR)} \end{cases}$
$\nu_2$ ( $E$ ) (R)	2A (IR, R)	$\begin{cases} 6(\text{Ag} + \text{B1g} + \text{B2g} + \text{B3g}) \text{ (R)} \\ 6(\text{B2u} + \text{B3u} + \text{B1u}) \text{ (IR)} \\ \text{Au (i)} \end{cases}$
$\nu_3, \nu_4$ ( $F_2$ ) (IR, R)	3A (IR, R)	$\begin{cases} 9(\text{Ag} + \text{B1g} + \text{B2g} + \text{B3g}) \text{ (R)} \\ 9(\text{B2u} + \text{B3u} + \text{B1u}) \text{ (IR)} \\ \text{Au (i)} \end{cases}$

IR, infrared active; R, Raman active; i, inactive.

dates are not observed in this zone, while the tetrahedron and octahedron modes can easily be seen. This behaviour is also different from that of the molybdates of trivalent cations, including the transition ones [13] to which the assignation of the  $\nu_1$  and  $\nu_3$  modes is difficult owing to the strong couplings observed, and because the  $\text{M(III)O}_6$  modes cannot be determined. In this zone of the infrared and Raman spectra, our assignation is more reliable and the modes of both polyhedra can be perfectly appreciated.

In both spectra, in the low-frequency zone, two modes appear corresponding to  $\nu_2$  (symmetric deformation) and the three  $\nu_4$  modes (antisymmetric deformation) of  $\text{MoO}_4^{2-}$  as expected by site symmetry. In our Raman spectra,  $\nu_2$  appears at higher frequency and with more intensity than  $\nu_4$ , in contraposition to

TABLE II Assignment of the vibrational spectrum of  $\text{Lu}_2(\text{MoO}_4)_3$

$\text{MoO}_4$ (Td)			$\text{LuO}_6$ (Oh)		
Mode	IR	Raman	Mode	IR	Raman
$\nu_1$ ( $A_1$ )	960	956	$\nu_1$ ( $A_{1g}$ )		818
	990 (s)	995			
	935	944			
$\nu_3$ ( $F_2$ )	870	864	$\nu_2$ ( $E_g$ )		665
	860	844			
	805	797			
	770	789			
			$\nu_3, \nu_4$ ( $F_{1u}$ )	415 (s) <sup>a</sup>	
				400	
$\nu_2$ (E)	372 (s)	403			
	362	373			
$\nu_4$ ( $F_2$ )	345	343 (s)			
	335	336			
	330	324			
lattice modes	290		$\nu_5$ ( $F_{2g}$ )		290
	280				
		262			

<sup>a</sup> s: shoulder.

TABLE III Values of  $\nu_1$  of Raman spectra ( $\text{cm}^{-1}$ )

Type	Molybdate						
$\text{Sc}_2(\text{WO}_4)_3$	Tb	Dy	Ho	Er	Tm	Yb	Lu
	945	990	955	990	990	956	956
$\text{La}_2(\text{MoO}_4)_3$	La	Ce	Pr	Nd	Sm	Eu	Gd
	920	935	934	936	934	940	936

other authors who state that both modes are overlapped [14]. At the end, lattice modes also appear.

### 3.2.2. $\text{La}_2(\text{MoO}_4)_3$ lattices

Fig. 2 shows the infrared and Raman spectra of  $\text{Nd}_2(\text{MoO}_4)_3$  typical of this series; Table IV gives a possible assignation.

In the stretching zone, both in the infrared and Raman spectra, great splittings of the  $\nu_1$  and  $\nu_3$  modes are observed without being able to give a reliable assignation. This behaviour and the considerable intensity of the set of lines in the Raman spectra show the presence of strong couplings between the different polyhedra of the lattice, owing to the existence of very distorted tetrahedra in a highly condensed lattice.

For these phases, a linear behaviour of  $\nu_1$  is not observed either, with the effective nuclear charge of the cation (see Table III).

A similar behaviour is observed in the deformation zone owing to the fact that the tetrahedron  $\nu_2$  cannot be distinguished from  $\nu_4$  either. In this zone, the modes of the  $\text{LnO}_8$  polyhedra again cannot be convincingly assigned.

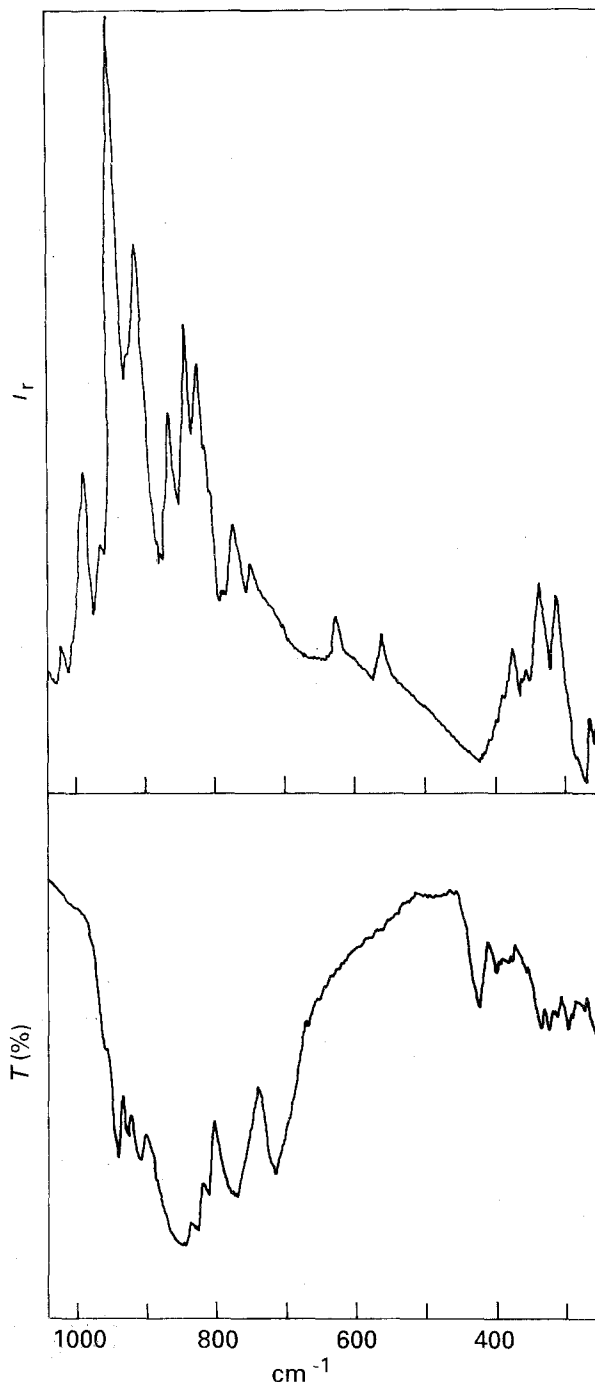


Figure 2 Vibrational spectrum of  $\text{Nd}_2(\text{MoO}_4)_3$ .

## 4. Conclusions

These materials with two different types of structure are clearly characterized by vibrational spectroscopy, as determined for other compounds with electrical [13] and catalytic properties [15].

In the  $\text{Sc}_2(\text{WO}_4)_3$  molybdates, the modes of both polyhedra could be assigned and the selection rules by sites symmetry are fulfilled.

In the  $\text{La}_2(\text{MoO}_4)_3$ -type molybdates, structures with vacancies and with distorted tetrahedra, couplings exist between the vibrational modes of both types of polyhedra of the highly condensed lattice.

The best catalytic activity of these compounds in the hydrogenation processes was found by

TABLE IV Assignment of the vibrational spectrum of  $\text{Nd}_2(\text{MoO}_4)_3$

$\text{MoO}_4$ (Td)			$\text{NdO}_8$ (polyhedral)		
Mode <sup>a</sup>	IR	Raman	Mode <sup>a</sup>	IR	Raman
		1194?			
		1096			
		1072			
$\nu_1$ ( $A_1$ )	940	936			
		986			
+	960 (s) <sup>b</sup>	961			
$\nu_3$ ( $F_2$ )	925	918			
		905			
+					
coupling	855	860	$\nu_{(\text{Nd}-\text{O})}$		839
	830	820			
	815	807			
	775	771			
		748			
	715	726	$\nu_{(\text{Nd}-\text{O})}$		629
					563?
			$\nu_{(\text{Nd}-\text{O})}$	425	
		392		400 (s)	
$\nu_2$ (E)	385 (s)	374			
	360 (s)	357			
+					
	340	335	$\nu_{(\text{Nd}-\text{O})}$		335
$\nu_4$ ( $F_2$ )	325				
	315 (s)	313			313
+					
coupling					
	300				
+	290 (s)				
lattice modes		262			

<sup>a</sup> with coupling.

<sup>b</sup> s, shoulder.

$\text{La}_2(\text{MoO}_4)_3$  molybdates with vacancies in the lattice [12].

### Acknowledgements

This work was supported by CONICET (PID 3076500 and PID 3-081400/88) and Universidad

Nacional de San Luis. The authors thank Dr Pedro J. Aymonino for facilitating the Raman spectrophotometer, and Lic. María E. López for linguistic advice.

### References

1. S. C. ABRAHAMS and J. L. BERMSTEIN, *J. Chem. Phys.* **45** (1966) 2745.
2. I. SUZUKI and Y. ISHIBASHI, *J. Phys. Soc. Jpn.* **56** (1987) 596.
3. V. MASSAROTTI, G. FLOR and A. MARINI, *J. Appl. Crystallogr.* **14** (1981) 64.
4. J. GRASSELLI, M. K. SNAVELY and B. J. BULKIN, "Chemical Applications of Raman Spectroscopy" (Wiley, New York, 1981).
5. E. J. BARAN, R. C. MERCADER, G. E. NARDA and J. C. PEDREGOSA, *Solid State Commun.* **58** (1986) 503.
6. M. A. JURI and J. C. PEDREGOSA, *Anal. Asoc. Quím. Argent.* **74** (1986) 509.
7. M. S. AUGSBURGER, M. A. JURI and J. C. PEDREGOSA, *ibid.* **77** (1989) 467.
8. C. A. ACOSTA, M. del C. VIOLA and J. C. PEDREGOSA, *J. Mater. Sci. Lett.* **10** (1991) 251.
9. L. H. BRIXNER and A. W. SLEIGHT, *Mater. Res. Bull.* **8** (1973) 1269.
10. W. JEITSCHKO, *Acta Crystallogr.* **B29** (1973) 2074.
11. P. TARTE and M. LIEGEOIS-DUYKAERTS, *Spectrochim. Acta* **28A** (1972) 2029.
12. M. A. JURI, Doctoral Thesis, UNSL (1988).
13. M. A. JURI, M. del C. VIOLA and J. C. PEDREGOSA, *Acta Sud Am. Quím.* **4** (1984) 37.
14. M. T. PAQUES-LEDENT and P. TARTE, *Spectrochim. Acta* **30A** (1974) 673.
15. M. MALLEA, J. RABA, S. QUINTAR, G. E. NARDA, V. CORTINEZ and J. C. PEDREGOSA, *J. Mater. Sci. Lett.* **8** (1989) 397.

Received 4 June 1992

and accepted 7 May 1993